Journal of Geotechnology and Energy | vol. 42 | no. 2 | 2025 | pp. 29–37

https://doi.org/10.7494/jge.2025.42.2.7116

ARTICLE

Jacek Blicharski

AGH University of Krakow, Faculty of Drilling, Oil and Gas, Poland
ORCID: 0000-0003-2082-6590
e-mail: jblich@agh.edu.pl

Izabela Dybaś

Independent Researcher
Polska Spółka Gazownictwa sp. z o.o.
ORCID: 0009-0005-0275-031X
e-mail: izabela.dybas@psgaz.pl

THE IMPACT OF RESERVOIR PARAMETERS AND WELL CONSTRUCTION ON GAS WELL PRODUCTIVITY

Date of submission:
27.03.2025

Date of acceptance:
10.04.2025

Date of publication:
30.06.2025

https://journals.agh.edu.pl/jge

Abstract: The aim of this paper was to present the influence of selected reservoir parameters and well construction on the productivity of a gas well, using the example of a natural gas reservoir with high nitrogen content. Data from an exemplary well were used to carry out a variant assessment of the productivity of wells at different stages of reservoir exploitation, taking into account single- and two-phase gas-condensate mist flow in the well. The reservoir development process is briefly described at the beginning. Subsequently, the issues of gas inflow to the well, gas flow in the well and nodal analysis were discussed. The last part of the paper focuses on the variant assessment of the productivity at different stages of reservoir exploitation using a computational algorithm for single-phase and two-phase gas-condensate mist flow in the well.

Keywords: nitrogen gas reservoir, gas well productivity, deliverability, inflow performance relationship, vertical lift performance, nodal analysis

1. Introduction

Natural gas is a raw material playing a significant role in the energy and chemical industries. A discovered natural gas reservoir is characterized by the following parameters: initial pressure, reservoir thickness, porosity, permeability, reservoir temperature and the composition of the reservoir fluid. Based on these criteria which define the reservoir, it is possible to determine whether there are balance resources and then under economic and technical conditions, industrial resources [1]. Once industrial resources of natural gas are confirmed, the hydrocarbon reservoir is developed. The well or wells providing access to the reservoir are tested with a tubular reservoir sampler. Subsequently, the well is secured both internally and at the surface. A production string is lowered into the production casing, enabling the flow of reservoir fluid from the bottom of the well to the surface while protecting the production casing from the effects of high reservoir pressure and the components of gas that contribute to corrosion and damage to the inner walls of the pipes. A production tree is attached to the production string, which serves as the surface security of the well and simultaneously allows connection to a system designed for receiving and treating the reservoir fluid. Before the commencement of reservoir exploitation, each well is tested to determine its production capacity [2].

The productivity of a gas well is the maximum amount of gas that can be extracted from the reservoir using a well in a given time, most often expressed in units of Scm/s (m^3 of gas at standard conditions per second). It depends on the geological parameters of the reservoir, in particular on the reservoir pressure, the permeability and thickness of the reservoir, as well as on the well parameters, such as the diameter of the production pipes used to access the reservoir. The efficiency of the well also depends on the composition of the reservoir fluid itself, including its viscosity and density, which affects its flow through the rock medium [3].

There are two fields of high nitrogenous natural gas in Poland. These reservoirs are called Sulęcin and Cychry. One of them, Cychry, is localized in the Polish Lowland. The gas is composed of over 90% nitrogen and this reservoir is accessed by two wells which have a similar construction and depth [4].

In order to determine optimal extraction, obtain information on reservoir parameters and determine the production zones of a given reservoir, hydrodynamic tests are performed, consisting of the creation of a state of non-equilibrium in the well while simultaneously measuring the reaction of the reservoir to the pressure disturbance that occurs in it. The reaction of the reservoir is recorded by measuring pressure changes over time [5].

2. Methodology

2.1. Gas inflow to the well

The gas inflow to the well can be described by the reservoir performance curve, abbreviated as the "IPR curve – Inflow Performance Relationship", which is a function of the relationship between the pressure at the bottom of the well and the flow rate. It is determined based on the gas inflow equation (1) named two-term formula [6]:

$$p_{bh} = \sqrt{p_r^2 - \frac{\mu \cdot z \cdot p_{sc} \cdot T}{\pi \cdot k \cdot h \cdot T_{sc}} \cdot \left(\ln \frac{r_e}{r_w} - \frac{3}{4} + S_m \right) \cdot q} \cdot \sqrt{- \frac{\mu \cdot z \cdot p_{sc} \cdot T}{\pi \cdot k \cdot h \cdot T_{sc}} \cdot D_t \cdot q^2} \tag{1}$$

where:

p_{bh} – bottomhole pressure [Pa],
p_r – average reservoir pressure [Pa],
q – gas flow rate [Scm/s],
k – reservoir permeability [m^2],
μ – gas viscosity [Pa·s],
z – gas compressibility factor [–],
p_{sc} – pressure at standard conditions [Pa],
T – reservoir temperature [K],
T_{sc} – temperature at standard conditions [K],
r_e – outer boundary radius [m],
r_w – wellbore radius [m],
S_m – mechanical skin factor [–],
h – reservoir thickness [m],
D_t – turbulence coefficient [s/m^3].

In a simplified form, this formula appears as follows:

$$p_{bh} = \sqrt{p_r^2 - a \cdot q - b \cdot q^2} \tag{2}$$

where:

$$a = \frac{\mu \cdot z \cdot p_{sc} \cdot T}{\pi \cdot k \cdot h \cdot T_{sc}} \cdot \left(\ln \frac{r_e}{r_w} - \frac{3}{4} + S_m \right)$$

$$b = \frac{\mu \cdot z \cdot p_{sc} \cdot T}{\pi \cdot k \cdot h \cdot T_{sc}} \cdot D_t$$

Figure 1 shows well inflow performance curves for different values of the product of permeability and reservoir thickness.

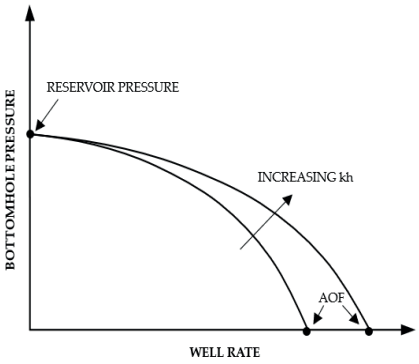

Fig. 1. Well inflow performance curves [7]

The analysis of Figure 1 shows that for zero well rate, the dynamic bottomhole pressure is equal to the average reservoir pressure. With the decrease of the bottomhole pressure the well rate increases until the bottomhole pressure reaches a value equal to atmospheric pressure, then the well rate takes on a maximum value, i.e. the potential well deliverability called "AOF", which can also be determined as a positive root of the equation of the two-term formula (1) [7]:

$$AOF = \frac{-a + \sqrt{a^2 + 4 \cdot b \cdot (p_r^2 - p_{sc}^2)}}{2 \cdot b} \tag{3}$$

From the equation (2) describing the IPR curve, it can be concluded that the slope of this curve is inversely proportional to the product of the thickness (h) and the permeability of the reservoir (k). With the increase of the product kh, the IPR curve becomes flatter.

2.2. Tubing-flow performance

The well flow rate in a well refers to the pressure drop as a function of the gas flow rate in the well. It depends on the well configuration and the properties of the transported fluid. For a single-phase gas flow in a well with constant parameters, i.e.: cross-section area, temperature, compressibility coefficient and friction, the tubing performance equation has the form [6]:

$$p_{bh} = \sqrt{p_{wh}^2 \cdot e^{\frac{2 \cdot g \cdot H}{z \cdot R \cdot T}} + \frac{8 \cdot \lambda \cdot p_{sc}^2 \cdot z^2 \cdot T^2 \cdot \left(e^{\frac{2 \cdot g \cdot H}{z \cdot R \cdot T}} - 1\right) \cdot q^2}{\pi^2 \cdot T_{sc}^2 \cdot D^5 \cdot g}} \tag{4}$$

where:

p_{wh} – wellhead pressure [Pa],
g – gravitational constant [m/s^2],
H – wellbore depth [m],
R – individual gas constant [J/kg·K],
λ – friction factor [–],
D – tubing diameter [m].

Equation (4) consists of two parts: I static – expresses the pressure of the gas column in the well and II dynamic – determines the pressure loss due to overcoming the gas flow resistance in the well.

Gas well streams can contain some liquid condensate which is usually dispersed in the gas in the form of mist. The flowing mixture of gas and condensate can be treated as a pseudo-homogeneous fluid with corresponding properties of the single phase recombined hydrocarbon fluid, i.e. the fluid obtained from recombining the well stream gas and liquid in the same proportion as they are produced. This implies that the flow behavior of a gas-condensate mixture in a wellbore can be described using single-phase flow models, as long as appropriate adjustments and modifications are made to account for the properties of the pseudo-homogeneous fluid.

In the case of two-phase gas-condensate mist flow, the equation is as follows [7]:

$$p_{bh} = \sqrt{p_{wh}^2 \cdot e^{\frac{2 \cdot g \cdot M_g \cdot H}{z_g \cdot R_u \cdot T}} + \frac{8 \cdot \lambda \cdot R_u \cdot p_{sc}^2 \cdot z^2 \cdot T^2}{M_g^2 \cdot \pi^2 \cdot T_n^2 \cdot D^5 \cdot g} \cdot \sqrt{\left(e^{\frac{2 \cdot g \cdot M_g \cdot H}{z_g \cdot R_u \cdot T}} - 1\right) \cdot \left(\rho_n \cdot q \cdot \left(1 + \frac{R_{VLG} \cdot \rho_L}{\rho_n}\right)\right)^2}} \tag{5}$$

where:

M_g – molecular mass of recombined gas [kg/kmol],
z_g – compressibility factor of recombined gas [–],
R_{VLG} – volumetric condensate/gas ratio (q_L/q_{sc}),
ρ_n – gas density at standard condition [kg/m^3],
R_u – gas constant [8314 joule/kmol·K],
ρ_L – condensate density [kg/m^3].

Figure 2 shows the well performance curves (VLP) for two different values of tubing diameters.

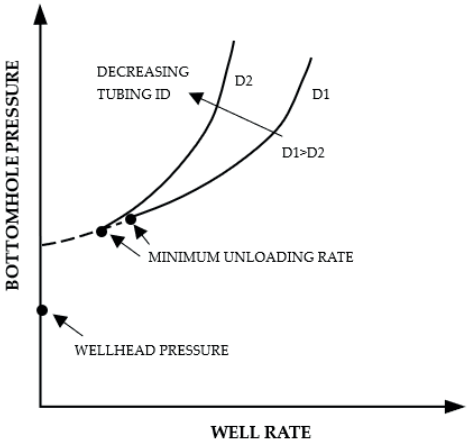

Fig. 2. Tubing flow performance [7]

Figure 2 shows VLP curves, depending on the bottomhole operating pressure from the well deliverability for different well tubing diameters at the assumed constant wellhead pressure. With the increase in the flow rate, the bottomhole operating pressure also increases and the curves deflect upwards, which is caused by the increasing flow resistance. The smaller the diameter of the tubing, the greater the flow resistance.

2.3. Nodal analysis

To determine the flow rate, nodal analysis is used, i.e. solving the system of equations for gas inflow to the well (1) and the well tubing performance equation (4) or (5). This solution can also be obtained graphically by intersecting the well performance curve (VLP) and the inflow performance curve (IPR) on a graph of p_{bh} versus q. The point at which these curves intersect determines the well deliverability, which is illustrated in Figure 3.

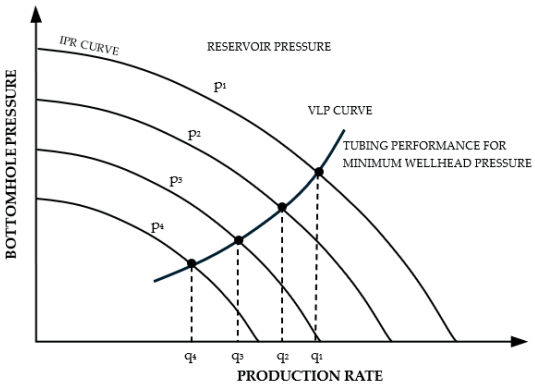

Fig. 3. Graphical determination of well deliverability using nodal analysis [7]

Figure 3 shows several IPR curves for different reservoir pressures and one VLP curve for the given wellhead pressure. These curves define several intersection points that determine the change in well performance with decreasing reservoir pressure and therefore the decrease in well production rates.

3. Calculations

Nodal analysis was used to perform variant assessment of the productivity of the well. First, calculations were made for IPR curves at three different reservoir pressures 55.13 MPa (initial reservoir pressure), 40 MPa, 30 MPa and three different reservoir permeabilities 16.2 mD, 12.1 mD, 8.1 mD. Having assumed the coefficients "a" and "b" of the two-term formula, their values were corrected due to the change in gas properties with pressure and the change in phase permeability. Permeability was reduced because with the decrease in pressure in the gas-condensate reservoir, condensate is deposited in the reservoir pores, which results in a decrease in the effective reservoir permeability.

In the next stage of calculations, VLP well performance curves were constructed for different wellhead pressures 30 MPa, 20 MPa and 12 MPa and two tubing diameters 2 7/8″ and 3 1/2″.

A multi-variant analysis was conducted to assess gas well productivity. This analysis allows for the evaluation of the impact of the a.m. parameters on the well deliverability.

The Soave–Redlich–Kwong equation was used to calculate the gas compressibility factor "Z", while the gas viscosity was determined using the Lee–Gonzalez correlation.

3.1. Data and calculation assumptions

The calculations were based on the assumed input data collected in Tables 1 and 2.

Table 1 . Composition and parameters of gas

Composition	Symbol	Molecular vol. [%]	Critical pressure [MPa]	Critical temperature [K]	Molecular mass [kg/kmol]	Acentric coefficient [–]
Methane	CH_4	5.174	4.641	190.55	16.042	0.008
Ethane	C_2H_6	1.290	4.913	305.50	30.068	0.980
Propane	C_3H_8	0.951	4.264	369.80	369.8	0.152
nButane	n-C_4H_{10}	0.292	3.796	425.17	425.17	0.193
iButane	i-C_4H_{10}	0.120	3.647	408.14	408.14	0.176
nPentane	n-C_5H_{12}	0.202	3.374	469.78	469.78	0.251
iPentane	i-C_5H_{12}	0.200	3.333	462.96	462.96	0.197
Hexane	C_6H_{14}	0.178	3.031	507.86	507.86	0.296
Azote	N_2	90.868	3.396	126.25	126.25	0.040
Carbon dioxide	CO_2	0.555	7.382	304.19	304.19	0.225
Hydrogen sulfide	H_2S	0.170	8.940	373.20	373.20	0.081

Table 2. Parameters of the well and gas properties

Parameter	Value
Depth [m]	3,333
Initial reservoir temperature [°C]	111.3
Initial reservoir pressure [MPa]	55.13
Rock permeability [mD]	16.15
Tubing diameter [in]	2 7/8
Roughness of tubing [mm]	0.015
Thickness of the reservoir [m]	30
Condensate exponent [l/m^3]	0.089
Condensate density [g/cm^3]	0.7289
Condensate density under normal conditions [kg/m^3]	1.411
Coefficient "a" of two-term formula [MPa^2/(*Scm*/min)]	0.561236295
Coefficient "b" of two-term formula [MPa^2/(*Scm*/min)^2]	$7.90858 \cdot 10^{-5}$
Pseudo-reduced temperature [K]	174.339
Pseudo-reduced pressure [MPa]	4.091
Molecular mass of gas [kg/kmol]	31.571
Gas compressibility factor "Z" at initial conditions	1.3938
Gas viscosity at initial conditions [Pa · s]	$5.296 \cdot 10^{-5}$

4. Results

As a result of the variant calculations conducted for the well, gas flow rates were determined and are presented in Tables 3–7. The constructed VLP curves are shown in Figures 4–8 and the graphical solution of the nodal analysis for each variant is also presented in these figures. The intersection points indicate the target gas well productivity for the considered variants I–V. The individual variants differed in terms of the adopted reservoir pressures, wellhead pressures, reservoir permeabilities and tubing diameters.

The values for the variants are presented in Tables 3–7.

Variant I – single-phase gas flow

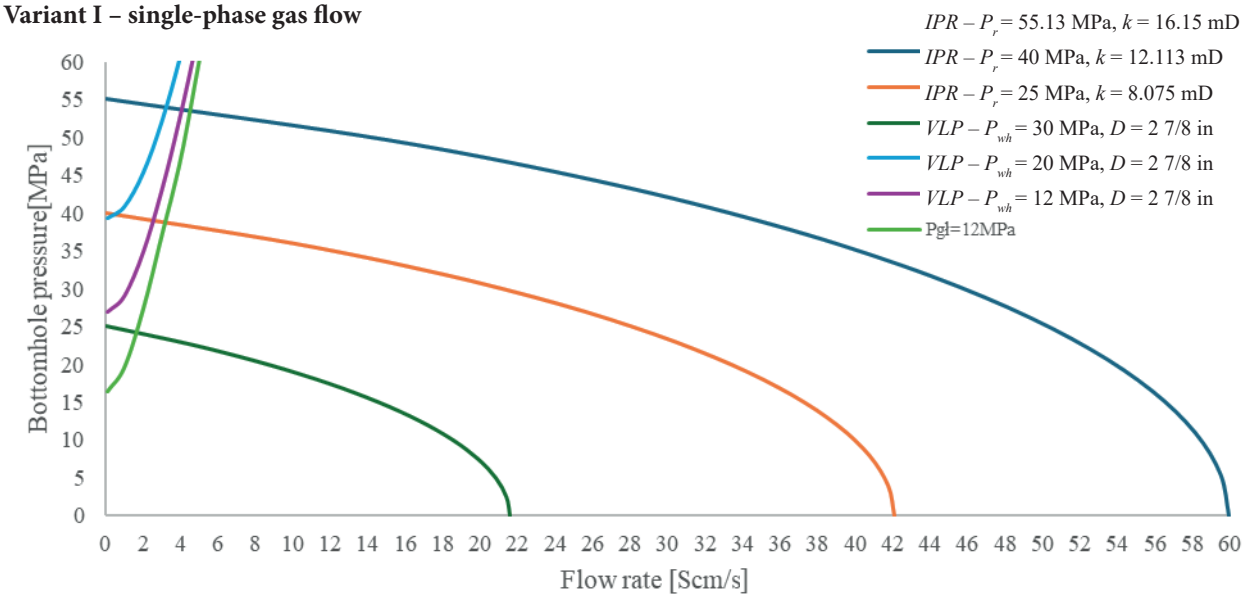

Fig. 4. IPR and VLP curves in variant I

Table 3. Well deliverability determined from the nodal analysis (variant I)

P_r [MPa]	P_{wh} [MPa]	*D* [in]	*k* [mD]	*q* [Scm/s]
55.13	30	2 7/8	16.15	**3.1**
55.13	20	2 7/8	16.15	**4**
55.13	12	2 7/8	16.15	**4.4**
40	30	2 7/8	12.113	**0.4**
40	20	2 7/8	12.113	**2.7**
40	12	2 7/8	12.113	**3.1**
25	12	2 7/8	8.075	1.8

Variant II – single-phase gas flow

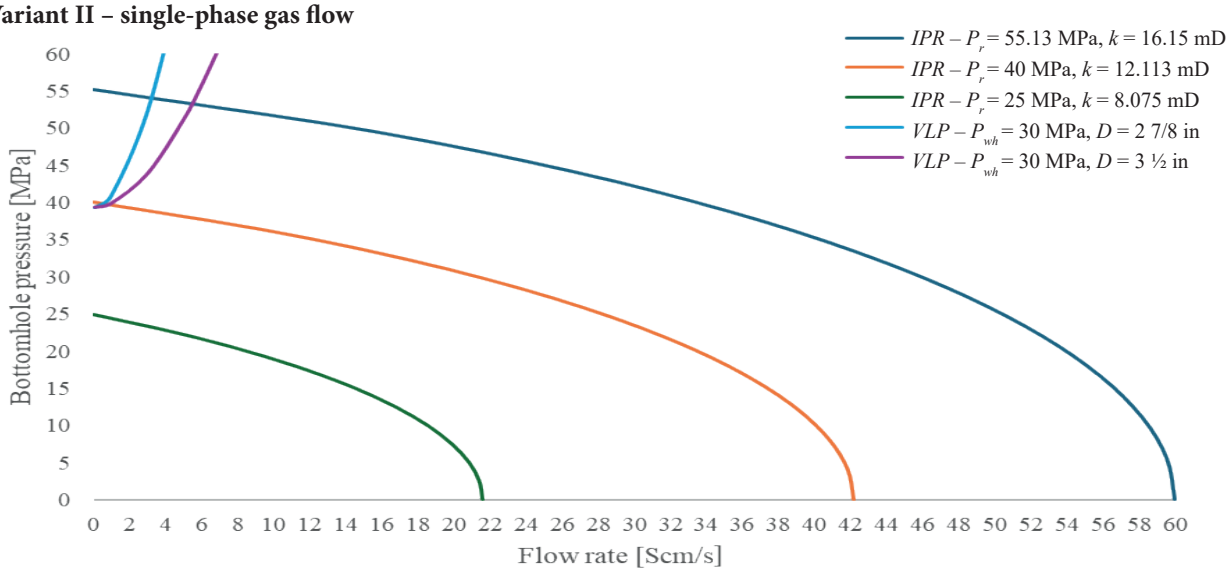

Fig. 5. IPR and VLP curves in variant II

Table 4. Well deliverability determined from the nodal analysis (variant II)

P_r [MPa]	P_{wh} [MPa]	D [in]	k [mD]	q [Scm/s]
55.13	30	2 7/8	16.15	**3.2**
55.13	30	3 1/2	16.15	**5.4**
40	30	2 7/8	12.113	**0.6**
40	30	3 1/2	12.113	**1**

Variant III – single-phase gas flow

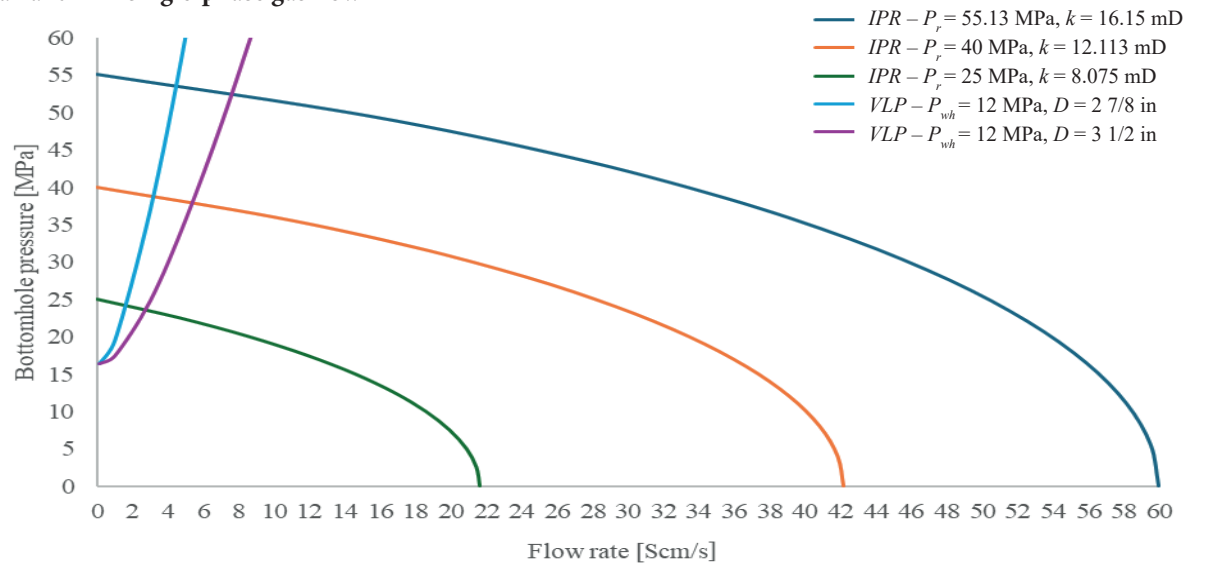

Fig. 6. IPR and VLP curves in variant III

Table 5. Well deliverability determined from the nodal analysis (variant III)

P_r [MPa]	P_{wh} [MPa]	D [in]	k [mD]	q [Scm/s]
55.13	12	2 7/8	16.15	**4.4**
55.13	12	3 1/2	16.15	**7.7**
40	12	2 7/8	12.113	**3.1**
40	12	3 1/2	12.113	**5.3**
25	12	2 7/8	8.075	**1.6**
25	12	3 1/2	8.075	2.8

Variant IV – two-phase gas-condensate mist flow

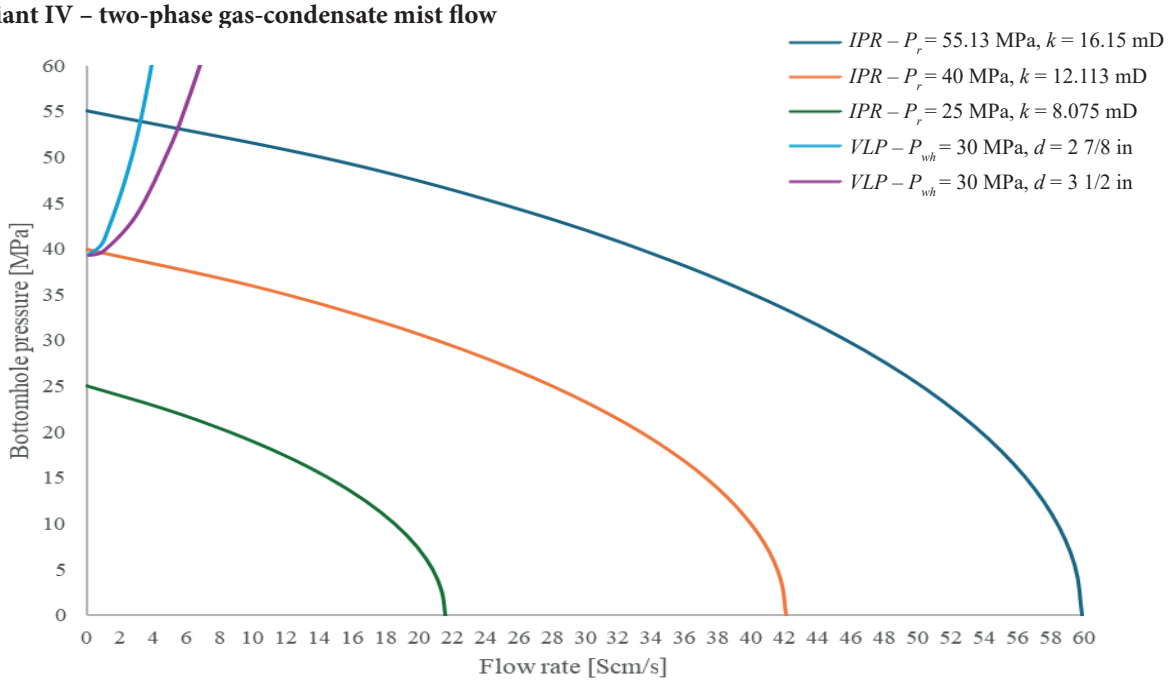

Fig. 7. IPR and VLP curves in variant IV

Table 6. Well deliverability determined from the nodal analysis (variant IV)

P_r [MPa]	P_{wh} [MPa]	D [in]	k [mD]	q [Scm/s]
55.13	30	2 7/8	16.15	**3**
55.13	30	3 1/2	16.15	**5.2**
40	30	2 7/8	12.113	**0.4**
40	30	3 1/2	12.113	**0.7**

Variant V – two-phase gas-condensate mist flow

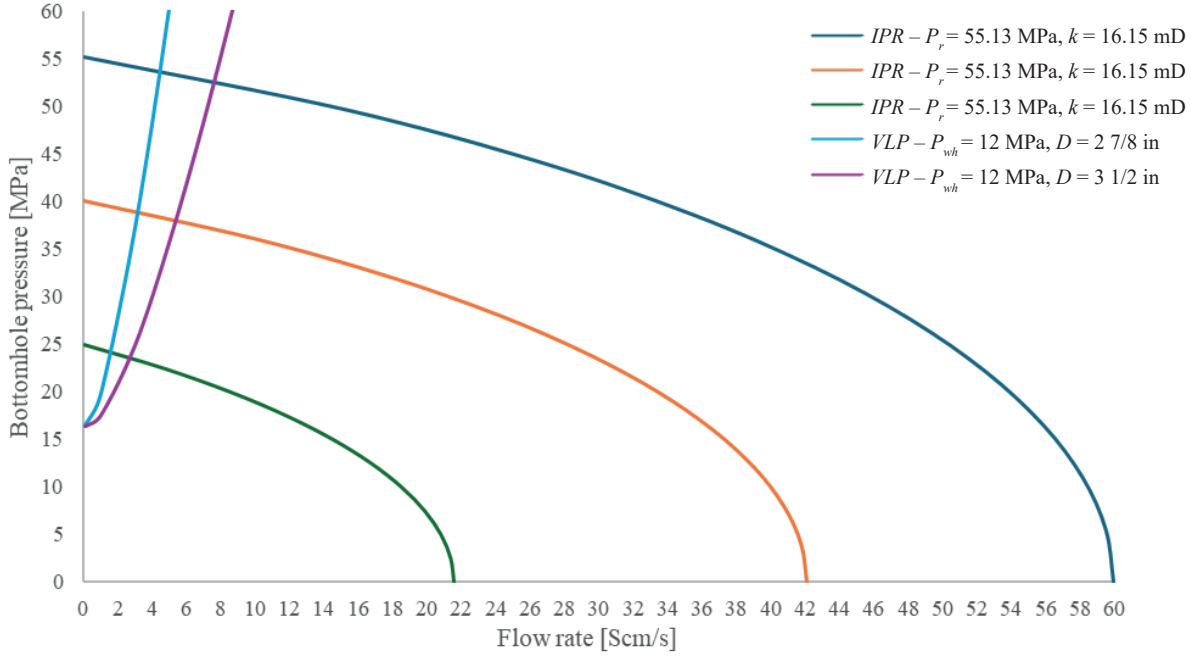

Fig. 8. IPR and VLP curves in variant V

Table 7. Well deliverability determined from the nodal analysis (variant V)

P_r [MPa]	P_{wh} [MPa]	D [in]	k [mD]	q [Scm/s]
55.13	12	2 7/8	16.15	**4.2**
55.13	12	3 1/2	16.15	**7.3**
40	12	2 7/8	12.113	**3**
40	12	3 1/2	12.113	**5.1**
25	12	2 7/8	8.075	**1.5**
25	12	3 1/2	8.075	**2.6**

4.1. Analysis of the results

In variant I, the well deliverability was determined at the formation pressures of 55.13 MPa (initial reservoir pressure), 40 MPa and 25 MPa, and wellhead pressures of 30 MPa, 20 MPa and 12 MPa, with a constant diameter of the production pipes of 2 7/8 in. The highest well deliverability was obtained at the initial formation pressure and the lowest wellhead pressure (12 MPa), which was 4.4 Scm/s. The calculations show that well deliverability decreases with a decrease in reservoir pressure and is lower at higher wellhead pressures.

In variants II and III, the influence of the diameter of the production tubes on the productivity of the well was analyzed. Higher well deliverability was obtained for a larger diameter of the production tubes and lower values of the wellhead pressure. The highest well deliverability was obtained in variant 3 for the diameter of the production tubes 3 1/2 in at the initial pressure and the wellhead pressure of 12 MPa and it amounted to 7.7 Scm/s.

Variants IV and V are modifications of variants II and III. In these variants, two-phase gas and condensate flow in the well was considered. The obtained results indicate a slight decrease in the well deliverability in both variants, i.e. IV and V, compared to variants II and III, which is caused by a greater pressure loss on the fluid flow in the well. In turn, this is caused by the increase in the gas column pressure and greater gas flow resistance with the condensate. The highest well deliverability value was obtained in variant V at a formation pressure of 55.13 MPa and a wellhead pressure of 12 MPa. In these conditions, the efficiency reached 7.3 Scm/s and was 5.2% lower compared to variant III. In variant IV, at an initial pressure of 55.13 MPa, the maximum well deliverability of 5.2 Scm/s was achieved, which was 3.7% lower compared to variant II.

5. Conclusions

The analysis conducted showed that the product of permeability and reservoir thickness has a significant impact on the productivity of the well; higher permeability enables easier filtration of the reservoir fluid, which results in higher flow rate.

Exploitation of the reservoir at a constant pressure value at the wellhead with decreasing reservoir pressure leads to a gradual decrease in well deliverability, limiting its productivity over time. Therefore, in order to maintain production at the required level, the wellhead pressure must also be gradually reduced. In turn, the minimum value of the wellhead pressure is dependent on the parameters of the gas received from the natural gas plant. In the variant calculations for the construction of the well deliverability curves, three different wellhead pressures were assumed: 30 MPa, 20 MPa, 12 MPa. The highest well deliverability was obtained for the lowest pressure at the wellhead of 12 MPa, at which the difference between the reservoir pressure and the wellhead pressure is the largest.

The diameter of the well tubing also has a significant impact on the productivity of the well, which translates into pressure loss during gas flow in the pipe and consequently into the flow rate. Two tubing diameters were assumed in the calculations: 3 1/2 in and 2 7/8 in. For a larger diameter of the tubing, the flow resistance is smaller, which means that the pressure loss during flow is smaller and consequently the well deliverability is higher. However, from the point of view of liquid unloading from the bottom of the well, with a smaller diameter of the tubing's, the gas flow rate is higher and the conditions for extracting the liquid phase from the well are more favorable. This is particularly important in the final phase of reservoir exploitation when the reservoir pressure is low and more water flows into the well, as well as condensate drops from the gas.

A comparative analysis of single-phase gas flow variants was carried out and two-phase mist (gas – condensate) in the well showed that, in the case of two-phase flow, the resistance to fluid flow in the well is higher, which is associated with a greater pressure loss caused by higher flow resistance and higher pressure of the fluid column in the well, which in turn translates into a decrease in the productivity of the well.

Author contributions: Conceptualization, formal analysis, methodology J.B., writing – review and editing, writing – original draft preparation, and investigation, I.D.; supervision, validation, project administration, J.B. All of the authors have read and agreed to the published version of the manuscript.

Funding: This research received no external funding.

Conflicts of Interest: The authors of this paper declares no conflicts of interest.

References

[1] Nieć M.: *Hydrocarbon resources classification: Polish, PRMS, UNFC and applied to shale gas. A comparison*. Nafta-Gaz, 9, 2016, pp. 715–716.
[2] Wolan M.: *Technical and technological solutions for the final equipment of wells with a deviated and horizontal section in wells in the Polish Lowlands*. Nafta-Gaz, 8, 2021, pp. 532–535.
[3] Guo B.: *Well Productivity Handbook*. University of Louisiana at Lafayette, Lafayette, LA, United States, 2019.
[4] *High nitrogenous natural gas*, https://www.pgi.gov.pl/en/1239-surowce/surowce/energetyczne/13954-high-nitrogenous-natural-gas.html [10.03.2025].
[5] Dake L.P.: *Fundamentals of Reservoir Engineering.* Elsevier, 1978.
[6] Nagy N. (red.): *Vademecum gazownika, T. 1: Podstawy gazownictwa ziemnego: pozyskiwanie, przygotowanie do transportu, magazynowanie.* Stowarzyszenie Naukowo-Techniczne Inżynierów i Techników Przemysłu Naftowego i Gazowniczego, Kraków 2014.
[7] Hagoort J.: *Fundamentals of Gas Reservoir Engineering*. Elsevier Science, 2012.
[8] Blicharski J.: *Modelowanie analityczne procesu magazynowania gazu w częściowo sczerpanych złożach gazu ziemnego – wybrane zagadnienia*. Wydawnictwa AGH, Kraków 2018.